

Global and comparative protein profiles of the pronotum of the southern pine beetle, *Dendroctonus frontalis*

O. Pechanova*, W. D. Stone†, W. Monroe‡,
T. E. Nebeker†, K. D. Klepzig§ and C. Yuceer*

*Department of Forestry, Mississippi State University, Mississippi State, MS 39762 USA; †Department of Entomology and Plant Pathology, Mississippi State University, Mississippi State, MS 39762 USA; ‡Electron Microscope Center, Mississippi State University, Mississippi State, MS 39762 USA; and §USDA Forest Service, Southern Research Station, 2500 Shreveport Highway, Pineville, LA 71360 USA

Abstract

The southern pine beetle (*Dendroctonus frontalis* Zimmermann) kills all pines within its range and is among the most important forest pest species in the US. Using a specialized mycangium surrounded by gland cells in the pronotum, adult females culture, transport, and inoculate two fungi into beetle galleries during oviposition. These fungal symbionts, to varying degrees, exclude antagonistic fungi and provide nutrients to larvae. However, the mechanisms (e.g. secreted antibiotic chemicals or nutrients, proteins or pathways) by which this relationship is maintained are not known. Here we present the first global and differential proteome profile of the southern pine beetle pronotum. Two-dimensional polyacrylamide electrophoresis, tandem mass spectrometry, and database searches revealed that the majority of pronotal proteins were related to energy-yielding metabolism, contractile apparatus, cell structure, and defence. The identified proteins provide important insights into the molecular and biochemical processes of, and candidates for functional genomics to understand mycangia and pronotum functions in, the southern pine beetle.

Keywords: southern pine beetle, *Dendroctonus frontalis*, pronotum, mycangium, proteomics, differential gel electrophoresis.

Introduction

The southern pine beetle (SPB), *Dendroctonus frontalis* Zimmermann (Coleoptera: Scolytidae) (Wood, 2007), is the most economically and ecologically important insect pest of southern forests in the U.S. (Drooz, 1985; Pye *et al.*, 2004). These tree killing bark beetles exhibit a mutualistic symbiotic relationship with two species of fungi: *Entomocorticium* sp. A and *Ceratocystiopsis ranaculosus* Hausner (Barras & Perry, 1972; Barras & Taylor, 1973; Happ *et al.*, 1976; Hsiau & Harrington, 1997; Hsiau & Harrington, 2003; Jacobs & Kirisits, 2003). The adult female SPB possesses a cuticular invagination called a mycangium in the pronotum within the thorax, whereas adult males form non-functioning pseudomycangia (Happ *et al.*, 1971). It is from this structure that *C. ranaculosus* and *Entomocorticium* sp. A are cultured, transported, and inoculated by females into beetle galleries during oviposition. The fungi subsequently proliferate in tree phloem tissues with the resulting hyphal mass providing essential nutrients to larvae (Klepzig *et al.*, 2001).

Female pronotal structures and metabolic pathways in mycangial gland cells appear to be key factors in selection and growth of fungi through chemical secretions from glandular cells (Happ *et al.*, 1971). Because the gland cells differ in morphology (Type 1 and Type 2), it was speculated that the secretion from one gland cell-type (Type 1) regulates the species composition of the fungi via the biosynthesis of defensive chemicals, whereas the other gland cell-type (Type 2) provides nutrients for fungal growth and reproduction (Happ *et al.*, 1971). However, no research has yet been conducted to address this theory and neither the nature of these hypothesized chemicals or nutrients, nor the proteins and pathways potentially involved in these processes have been identified. To begin closing these gaps, our objective was to identify globally and differentially expressed proteins from the pronotal tissues of adult beetles.

Proteomics is a powerful tool for qualitative and quantitative analyses of proteins in living organisms. Proteomic analysis generally involves separation of a protein mixture from a biological source by two-dimensional (2-D) electrophoresis or liquid chromatography (LC) followed by identification of individual proteins by mass spectrometry (MS) and database searches. The availability of genome sequences for several

Received 11 December 2007; accepted after revision 30 January 2008.
Correspondence: Cetin Yuceer, Department of Forestry, Mississippi State University, Box 9681, Mississippi State, MS 39762, USA. Tel.: +1-662-325-2795; fax: +1-662-325-8726; e-mail: mcy1@ra.msstate.edu

insect species (Adams *et al.*, 2000; Holt *et al.*, 2002; The Honey Bee Genome Sequencing Consortium, 2006) has made proteomics a feasible means of studying insect proteins such as silkworm skeletal muscles (Zhang *et al.*, 2007) and secretions from hypopharyngeal glands in honeybees (Santos *et al.*, 2004). Since many insect species are transmitters of various pathogens, a number of studies have focused on this interaction to detect pathogen-responsive proteins (Biron *et al.*, 2006; Lefevre *et al.*, 2007; Scharlaken *et al.*, 2007).

Here we present the first 2-D protein reference map of SPB pronotal tissues. Moreover, we used comparative quantitative proteomics to identify differentially expressed proteins in female and male SPB pronotal tissues. Since no molecular level research on this important structure has been conducted, this study represents a launching step – description of pronotal proteome, which can serve as a foundation for future investigations. The identified proteins provide insights into the molecular and biochemical processes in the SPB pronotum which may be involved in maintaining the fungal symbiosis within the mycangium. Understanding the mutualistic relationship between female SPB and symbiotic fungi at the molecular level is expected

to contribute to molecular ecology and translate into practical significance of pest management strategies. This molecular interaction could be targeted for disruption to potentially control the infestation of trees by SPBs which are extremely difficult to control, and practically no effective pest management tactics have been developed.

Results and discussion

Morphology of the southern pine beetle pronotum

Using scanning and transmission electron microscopy, we examined the morphology of the female SPB pronotum to aid the interpretation of our global and comparative protein profile data. The mycangium is located at the anterior edge of the pronotum (a shield-shaped structure immediately behind the head) within the prothorax (Fig. 1). This specialized structure contains the inner wall of the pronotum and the anterior entothoracic fold. The mycangium is also surrounded by secretory cells with tracheoles and several efferent ductules which appear to be filled with a waxy secretory product. This apparently secreted product empties into the mycangial lumen. Other major components of this pronotal region include chitinous cuticle and muscles.

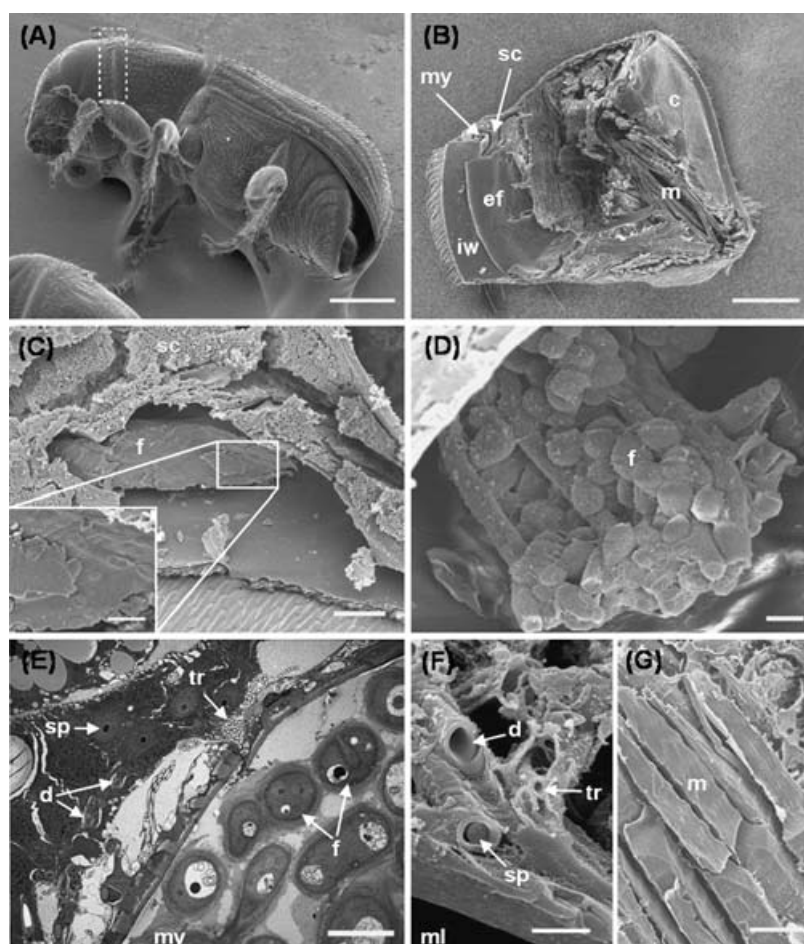


Figure 1. Electron micrographs showing the pronotal morphology and symbiotic fungi of female southern pine beetle. (A) The dotted line is drawn around the anterior region of the pronotum, below which the mycangium is located. (B) Sagittal view of the pronotum cross-section showing the inner wall (iw) and the anterior fold (ef) which surrounds the elongate mycangium (my) and various secretory cells (sc). Other major components of the pronotum are chitinous cuticle (c) and muscles (m). (C) Fractured mycangium whose lumen is filled with symbiotic fungi (f). The mycangium is surrounded by proximal and distal secretory gland cells. The inset shows the close up view of fungi. (D) Symbiotic fungi in the mycangial lumen. (E) Transmission electron micrograph showing a cross-section of the mycangium and surrounding gland cells. Efferent ductules (d) transport electron-dense secretory product (sp) to the mycangium. Present are also numerous tracheoles (tr) and symbiotic fungi. (F) Scanning electron micrograph showing tracheoles and several efferent ductules filled with secretory product. The secretory product empties into the mycangial lumen (ml). (G) Numerous muscles found within the pronotum. Bars: 500 μ m in A; 200 μ m in B; 20 μ m in C (5 μ m in inset); 2 μ m in D; 2 μ m in E; 1 μ m in F; 1 μ m in G.

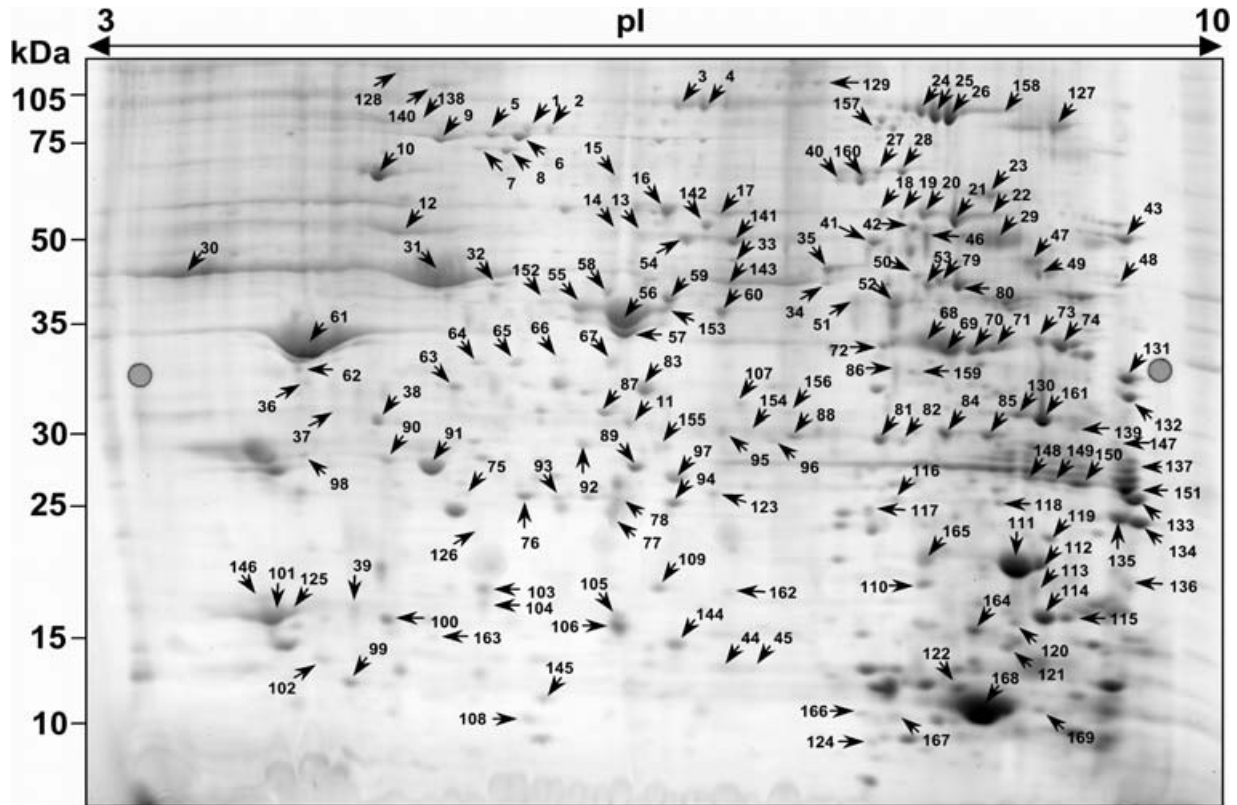


Figure 2. 2-D protein reference map of the SPB pronotum. Five hundred micrograms of proteins were first separated by isoelectric focusing on 24 cm IPG strip with non-linear 3–10 pH gradient (pI) and in second dimension on a large format 10–15% polyacrylamide gradient gel. Proteins were visualized with Deep Purple Total Protein Stain. Numbers and arrows indicate protein spots for which identity/similarity was obtained. Protein molecular weights are seen in kilo Daltons (kDa).

Global proteome profile of the southern pine beetle pronotum

The tissue we focused on is found within the middle of the three adult insect body segments. This region contains soft muscle mass and exoskeleton as well as the mycangia and surrounding gland cells in the female. Our 2-D proteome map is a reflection of these morphologies. Approximately 900 spots were visualized on Deep Purple stained 2-D gels of combined whole cell protein extracts from female and male SPB pronota (Fig. 2). The most abundant 266 protein spots were excised and analyzed. Using the red flour beetle (*Tribolium castaneum*) protein database, we obtained significant matches for 139 spots (Table 1). Additional 30 spots were identified using the National Center for Biotechnology Information (NCBI) non-redundant database (Table 2). Thus, identity for a total of 169 spots was obtained (a 63.5% identification success rate). Sequence similarity searches against UniProt Knowledgebase revealed that all the red flour beetle protein sequences had identifiable similar proteins in other insect species. For 75 distinct red flour beetle proteins, similar proteins were found in 23 different insect species. From those, 25 proteins had

the highest sequence similarity match to mosquito (*Aedes aegypti*), 16 proteins to silkworm (*Bombyx mori*), and 13 proteins to fruit fly species (*Drosophila* spp.). The degree of sequence similarity ranged from 40% to 100%. Thirty red flour beetle proteins had sequence similarity above 80%. Thirty-six proteins had 60% to 80% sequence similarity, whereas seven proteins showed sequence similarity below 60%. Regarding the NCBI database identifications, eight out of 21 positive hits corresponded to known proteins from eight different insect species, whereas 12 corresponded to unknown or predicted proteins. BLASTP search of the latter produced 64% to 100% sequence similarity in five insect species (yellow fever mosquito, honey bee, malaria mosquito, moth, and silkworm).

The majority of the protein spots were identified based on multiple peptide hits. However, proteins that matched with a single peptide (spots 110, 111, and 112 for muscle protein 20-like; spot 125 for ATP synthase delta chain; and spot 137 for GA20391-PA) were deemed acceptable as identifications since they met strict search criteria of total protein confidence interval > 95%. With one exception (spot 137), all single peptide hits corresponded to small proteins that have molecular mass close to or less than 20 kDa.

Table 1. List of proteins identified using the red flour beetle database

Spot number	<i>Tribolium</i> ID	Mr/pI* (kDa) (theoretical)	Number of matched peptides	Annotation/protein similarity	Sequence similarity**	Accession number	Organism
Metabolism							
24, 25, 26, 27, 28	GLEAN_05725	85.4/8.2	9, 11, 12, 7, 7	Aconitase, mitochondrial	82%	Q16KR4	<i>Aedes aegypti</i>
54	GLEAN_11730	48.1/8.7	7	Enolase	81%	Q7Q3D8	<i>Anopheles gambiae</i> str. PEST
51, 52	GLEAN_14998	39.7/7.6	6, 4	Fructose-bisphosphate aldolase	78%	Q6PPI0	<i>Homalodisca coagulata</i>
60	GLEAN_04962	42.3/7.5	8	Isocitrate dehydrogenase	79%	Q17P79	<i>A. aegypti</i>
67	GLEAN_11159	39.2/8.5	3	Pyruvate dehydrogenase	77%	Q17D51	<i>A. aegypti</i>
72	GLEAN_08177	35.8/8.7	4	Malate dehydrogenase	74%	Q171B2	<i>A. aegypti</i>
73, 74	GLEAN_15050	35.5/9.4	5, 4	Malate dehydrogenase	78%	Q16ZI5	<i>A. aegypti</i>
79, 80	GLEAN_14590	48.9/8.7	14, 13	NADPH-specific isocitrate dehydrogenase	77%	Q1HQ47	<i>Bombyx mori</i>
89	GLEAN_07346	26.8/7.0	6	Triosephosphate isomerase	86%	Q8MPF2	<i>Tenebrio molitor</i>
49	GLEAN_08872	50.9/9.2	4	Trifunctional enzyme beta subunit	72%	Q17IM1	<i>A. aegypti</i>
70, 71	GLEAN_05769	33.8/8.9	2, 4	3-hydroxyacyl-CoA dehydrogenase	65%	Q17H10	<i>A. aegypti</i>
58, 59	GLEAN_02547	45.8/8.5	6, 4	Probable medium-chain specific acyl-CoA dehydrogenase, mitochondrial precursor	81%	Q9VSA3	<i>Drosophila melanogaster</i>
127	GLEAN_14680	75.4/9.0	5	Hydroxyacyl-coenzyme A dehydrogenase	71%	Q2F686	<i>B. mori</i>
81, 82	GLEAN_05928	32.2/9.0	4, 5	Cyclohex-1-ene-1-carboxyl-CoA hydratase, putative	67%	Q17E10	<i>A. aegypti</i>
3, 4	GLEAN_04842	85.8/6.6	10, 11	Glutamate semialdehyde dehydrogenase	76%	Q174N2	<i>A. aegypti</i>
23	GLEAN_15385	63.0/8.7	5	Pyrroline-5-carboxylate dehydrogenase	77%	Q17A27	<i>A. aegypti</i>
55, 56, 57, 95, 96	GLEAN_13596	55.2/5.7	6, 6, 4, 8, 9	Arginine kinase	89%	A1KY39	<i>Periplaneta americana</i>
64, 65	GLEAN_04566	32.3/6.1	7, 5	Inorganic pyrophosphatase	68%	Q17G61	<i>A. aegypti</i>
Transport							
16	GLEAN_06823	15.9/5.2	3	Dihydrolipoamide dehydrogenase	82%	Q2LZ16	<i>Drosophila pseudoobscura</i>
108	GLEAN_06382	37.2/8.8	5	GA20735-PA	60%	Q28XR2	<i>D. pseudoobscura</i>
1, 2	GLEAN_06252	79.2/6.6	12, 10	NADH-ubiquinone oxidoreductase 75 kDa subunit	72%	Q16LR5	<i>A. aegypti</i>
12, 13	GLEAN_15322	55.2/5.2	18, 18	ATP synthase subunit beta	90%	Q1HPT1	<i>B. mori</i>
17, 18, 19, 20, 21, 22	GLEAN_08728	61.4/9.3	14, 10, 14, 9, 15, 8	Mitochondrial ATP synthase alpha subunit	90%	Q7PHI8	<i>A. gambiae</i> str. PEST
63	GLEAN_03690	27.1/5.9	5	NADH-ubiquinone reductase	68%	Q1HPR5	<i>B. mori</i>
83, 84, 85	GLEAN_08707	27.3/6.9	6, 7, 8	Electron-transfer-flavoprotein beta polypeptide	82%	Q2F6A1	<i>B. mori</i>
124	GLEAN_03304	10.9/7.7	3	Similar to <i>Drosophila melanogaster</i> CG14235	77%	Q6XHZ3	<i>Drosophila yakuba</i>
125	GLEAN_13931	16.6/5.1	1	ATP synthase delta chain, mitochondrial	71%	Q17I03	<i>A. aegypti</i>
135	GLEAN_00462	22.7/9.8	6	ATP synthase delta chain	66%	Q1HPX3	<i>B. mori</i>
Contractile apparatus							
29	GLEAN_07136	63.5/8.5	6	Muscle LIM protein	69%	Q2F677	<i>B. mori</i>
61, 62	GLEAN_11019	75.2/5.6	14, 16	Tropomyosin 1, isoforms 9A/A/B	64%	P06754	<i>D. melanogaster</i>
98, 99	GLEAN_11461	32.3/4.8	13, 9	Tropomyosin-1	87%	Q1HPU0	<i>B. mori</i>
101, 102	GLEAN_01048	20.4/5.1	5, 3	Myosin 2 light chain	71%	Q5MGI8	<i>Lonomia obliqua</i>
128	GLEAN_05924	262.3/5.5	39	Myosin heavy chain, nonmuscle or smooth muscle	81%	EAT42758	<i>A. aegypti</i>
109, 110, 111, 112	GLEAN_07135	20.3/8.9	2, 1,	Muscle protein 20-like protein	88%	Q4PLJ5	<i>Anoplophora glabripennis</i>
113	GLEAN_01139	20.3/9.0	6	Muscular protein 20	79%	Q1HPV5	<i>B. mori</i>
131, 132, 133	GLEAN_07015	36.8/9.7	8, 8, 5	Myofiliin protein	64%	Q0PKS0	<i>B. mori</i>
134, 135			7, 7				
Cytoskeleton organization							
30, 31, 32, 33,	GLEAN_03326	41.8/5.3	15, 21, 16, 10,	Actin	100%	Q5RLJ4	<i>Apriona germari</i>
34, 35, 36, 37,			15, 10, 11, 10,				
38, 39, 40, 41,			13, 14, 10, 8,				
42, 43, 44, 45			10, 10, 10, 10				

Table 1. Continued.

Spot number	<i>Tribolium</i> ID	Mr/pI* (kDa) (theoretical)	Number of matched peptides	Annotation/protein similarity	Sequence similarity**	Accession number	Organism
46, 47, 48	GLEAN_03944	41.8/5.3	11, 9, 9	Putative muscle actin	99%	Q6PPI5	<i>Homalodisca coagulata</i>
103, 104, 105, 106	GLEAN_01574	16.9/6.2	9, 5, 9, 9	Actin depolymerizing factor	91%	1HQF5	<i>A. aegypti</i>
114, 115	GLEAN_00431	19.0/8.7	2, 2	Calponin/transgelin	81%	Q16Z50	<i>A. aegypti</i>
129	GLEAN_05186	267.3/5.9	30	CHEERIO CG3937-PD, isoform D	64%	Q7KSF4	<i>D. melanogaster</i>
Detoxification and defence							
5, 6	GLEAN_00487	75.2/6.1	9, 8	Heat shock 70 kDa protein cognate 5	84%	P29845	<i>D. melanogaster</i>
7, 8	GLEAN_00188	69.0/5.6	10, 12	HSP70	83%	Q8I813	<i>Chironomus tentans</i>
9	GLEAN_02089	118.5/6.4	23	Heat shock cognate 70	89%	Q2WG65	<i>Plutella xylostella</i>
10, 11	GLEAN_13683	61.1/5.5	13, 7	60 kDa heat shock protein, mitochondrial precursor	81%	O02649	<i>D. melanogaster</i>
78	GLEAN_06793	20.8/6.5	4	Small heat shock protein 21	65%	Q3LGX2	<i>Gastrophysa atrocyanea</i>
90, 91, 92	GLEAN_01152	23.6/5.5	9, 8, 6	Heat shock protein 20.6	72%	Q0ZLZ3	<i>Locusta migratoria</i>
97	GLEAN_10105	21.8/6.2	4	Lethal (2)essential for life protein, l2efl	65%	Q16JF5	<i>A. aegypti</i>
122	GLEAN_13081	11.2/9.0	4	Heat shock protein, putative	72%	Q17MF2	<i>A. aegypti</i>
119	GLEAN_14505	23.1/8.2	3	Peptidyl-prolyl <i>cis-trans</i> isomerase	78%	Q9W227	<i>D. melanogaster</i>
93, 94	GLEAN_14929	21.8/6.3	7, 6	2-Cys thioredoxin peroxidase	79%	Q8WSF6	<i>A. aegypti</i>
116, 117	GLEAN_05780	23.6/8.3	2, 3	Superoxide dismutase	71%	Q65Y02	<i>B. mori</i>
123	GLEAN_12328	26.0/8.6	4	Thioredoxin peroxidase	65%	Q7YXM3	<i>Apis mellifera ligustica</i>
Protein metabolism							
100	GLEAN_09260	15.1/5.5	2	40S ribosomal protein S12	82%	Q6EUZ2	<i>Curculio glandium</i>
136	GLEAN_01004	17.0/10.2	5	Ribosomal protein S15e	92%	Q4GXQ7	<i>Micromalthus debilis</i>
137	GLEAN_11732	40.8/8.6	1	GA20391-PA	56%	Q298H4	<i>D. pseudoobscura</i>
14	GLEAN_06492	48.5/5.8	13	26S protease regulatory subunit	95%	Q16KL0	<i>A. aegypti</i>
53	GLEAN_10321	44.5/6.6	9	26S proteasome regulatory complex ATPase RPT4	94%	Q1HQM1	<i>A. aegypti</i>
107	GLEAN_00378	48.1/6.9	7	Leucine aminopeptidase	56%	Q17P99	<i>A. aegypti</i>
138	GLEAN_09174	89.1/5.3	13	Transitional endoplasmic reticulum ATPase TER94	89%	Q2V0H5	<i>B. mori</i>
120	GLEAN_15328	17.7/8.5	6	Ubiquitin carrier protein	93%	Q2Q469	<i>B. mori</i>
Signal transduction							
50	GLEAN_11700	36.7/5.8	7	GTP binding protein	81%	Q1HQC4	<i>B. mori</i>
66	GLEAN_14882	37.2/5.8	6	Guanine nucleotide-binding protein subunit beta-like	95%	A1YWY1	<i>Microplitis mediator</i>
86	GLEAN_06776	35.7/6.9	10	Receptor for activated protein kinase C-like	94%	Q09KA1	<i>Blattella germanica</i>
Nucleic acid metabolism							
15	GLEAN_10876	71.2/6.1	6	Dihydropyrimidinase	56%	Q171I2	<i>A. aegypti</i>
121	GLEAN_02492	17.2/9.2	5	Nucleoside diphosphate kinase	88%	Q1HP15	<i>B. mori</i>
75, 76, 77	GLEAN_14051	21.9/6.9	3, 5, 5	Probable adenylate kinase isoenzyme F38B2.4	65%	Q20140	<i>Caenorhabditis elegans</i>
139	GLEAN_04724	26.6/8.9	2	Dak2 protein	79%	Q9U915	<i>D. melanogaster</i>
137	GLEAN_08961	60.5/8.3	9	DNA polymerase iota	44%	Q175B7	<i>A. aegypti</i>
Regulation of transcription							
118	GLEAN_07692	65.0/7.5	7	High mobility group protein DSP1	46%	Q24537	<i>D. melanogaster</i>
Unclassified							
87, 88	GLEAN_13727	30.3/6.0	10, 9	Prohibitin protein WPH	87%	Q2F5J2	<i>B. mori</i>
68, 69	GLEAN_13758	46.5/8.0	11, 12	Four and a half lim domains	68%	Q17JP0	<i>A. aegypti</i>
126	GLEAN_10609	53.2/6.7	7	Focal contact protein paxillin	53%	Q9GSE0	<i>D. melanogaster</i>
130	GLEAN_11497	30.3/5.9	5	Transposase	40%	Q95US6	<i>Ceratitis rosa</i>

*Theoretical Mr and pI values were calculated using GPS software.

**Sequence similarity between red flour beetle protein and similar protein in UniProtKB.

Table 2. List of proteins identified using the NCBI database

Spot number	Protein identification (accession number) organism	Mr/pl* (kDa) (theoretical)	Number of matched peptides	Annotation/protein similarity	Sequence similarity**	Accession number	Organism
Metabolism							
141	Enolase (gi 53830714) <i>Oncometopia nigricans</i>	46.7/5.9	6				
157, 158	ENSANGP00000018525 (gi 55237854) <i>Anopheles gambiae str. PEST</i>	82.4/8.6	9, 13	Aconitase, mitochondrial	93%	Q16KR4	<i>Aedes aegypti</i>
159	GA18372-PA (gi 54639671) <i>Drosophila pseudoobscura</i>	82.0/8.3	10	Aconitase, mitochondrial	80%	Q16KR4	<i>A. aegypti</i>
152, 153, 154	PREDICTED: similar to arginine kinase (gi 66548235) <i>Apis mellifera</i>	43.6/6.4	11, 11, 8	Arginine kinase	99%	O61367	<i>Apis mellifera</i>
Transport							
156	ENSANGP00000021837 (gi 55238468) <i>Anopheles gambiae str. PEST</i>	45.4/8.3	7	Acyl-CoA dehydrogenase	89%	Q16GA1	<i>A. aegypti</i>
160	ENSANGP00000013487 (gi 55238706) <i>Anopheles gambiae str. PEST</i>	65.9/6.2	9	Electron transfer flavoprotein-ubiquinone oxidoreductase	87%	Q171U3	<i>A. aegypti</i>
161	PREDICTED: similar to CG6647-PA, isoform A isoform 2, (gi 91088623) <i>Tribolium castaneum</i>	30.2/8.3	8	Mitochondrial porin	71%	Q1HR57	<i>A. aegypti</i>
Contractile apparatus							
140	Muscle myosin heavy chain (gi 2546938) <i>Drosophila melanogaster</i>	138.5/5.5	29				
146	Troponin C2 (gi 56462266) <i>Lonomia obliqua</i>	16.9/3.9	3				
147	Troponin I-b1 (gi 38570287/Q6T2X4) <i>Drosophila subobscura</i>	29.7/9.7	11				
165	Muscle protein 20-like protein (gi 67527227/Q4PLJ5) <i>Anoplophora glabripennis</i>	20.3/7.8	4				
148, 149, 151, 152	PREDICTED: similar to ENSANGP00000025246 (gi 66504131/Q3B708) <i>Apis mellifera</i>	23.7/9.8	7, 8, 7, 9	Troponin I isoform 6a1	100%	Q3B708	<i>A. mellifera</i>
166, 167, 168, 169	PREDICTED: similar to LIM protein 1 (gi 66514669) <i>Apis mellifera</i>	10.1/8.6	3, 2 3, 3	LIM protein 1	90%	Q5MGJ0	<i>Lonomia obliqua</i>
Cytoskeleton organization							
143	Actin (gi 55783600/Q5RLJ4) <i>Apriona germari</i>	41.8/5.3	14				
145	Profilin (gi 56404766/Q68HB4) <i>Bombyx mori</i>	13.7/5.9	2				
Detoxification and defence							
144	Cu,Zn superoxide dismutase (gi 4103322) <i>Drosophila mimica</i>	14.9/5.8	3				
142	ENSANGP00000019291 (gi 55243618) <i>Anopheles gambiae str. PEST</i>	45.9/5.5	2	Brain chitinase and chia	83%	Q16M05	<i>A. aegypti</i>
164	ENSANGP00000020778 (gi 55243344) <i>Anopheles gambiae str. PEST</i>	18.0/8.7	3	Peptidyl-prolyl <i>cis-trans</i> isomerase	100%	Q7PS16	<i>Anopheles gambiae str. PEST</i>
162	PREDICTED: similar to Protein dodo (gi 66563115) <i>Apis mellifera</i>	18.1/7.0	2	Rotamase	69%	Q16UF6	<i>A. aegypti</i>
Protein metabolism							
155	ENSANGP00000015960 (gi 58391145) <i>Anopheles gambiae str. PEST</i>	27.6/6.2	6	Proteasome subunit alpha type	100%	Q7Q2B0	<i>A. gambiae str. PEST</i>
163	PREDICTED: similar to bendless CG18319-PA (gi 66564615) <i>Apis mellifera</i>	17.2/5.7	6	Ubiquitin carrier protein	98%	Q1HQ36	<i>B. mori</i>

*Theoretical Mr and pl values were calculated using GPS software.

**Sequence similarity between red flour beetle protein or unknown NCBI protein and similar protein in UniProtKB.

Many spots produced the same database matches, indicating protein spot redundancies. One hundred and sixty-nine identified protein spots corresponded to 96 unique gene products: 75 red flour beetle and 21 NCBI identifications. Fifty nine proteins were present in single spots. Only two spots (135 and 137) showed two different proteins, perhaps due to co-migration and inefficient separation on 2-D gel. All remaining 167 spots were singletons. The most abundant protein spots in terms of spot size and intensity corresponded to actin (spot 31), tropomyosin 1 isoform 9A/A/B (spot 61), muscle protein 20-like (spot 111), LIM protein 1 (spot 168), and arginine kinase (spot 56). Actin was found in 20 spots across the gels (spots 30 through 48, and spot 134), comprising 11.8% of the total identified spots. Other examples of spot redundancies were mitochondrial ATP synthase alpha subunit (spots 17, 18, 19, 20, 21, and 22) and arginine kinase (spots 55, 56, 57, 95, and 96). Mitochondrial aconitase (spots 24, 25, and 26) appeared to be glycosylated, showing a pattern in which a series of closely positioned spots drifted towards lower pI and higher molecular mass.

Physicochemical characteristics

Theoretical pI values of the identified proteins ranged from 3.93 to 10.21, and their theoretical molecular masses were from 10.1 to 267.3 kDa. The most acidic protein was troponin (spot 146; pI 3.93, theoretical), whereas the most basic was ribosomal protein S15e (spot 136; pI 10.21, theoretical). A significant portion of proteins were in the alkaline region of the gel. Four proteins had molecular mass higher than 100 kDa, such as myosin heavy chain, nonmuscle or smooth muscle protein (spot 128; 262.3 kDa), muscle myosin heavy chain (spot 140; 138.5 kDa), and heat shock cognate 70 (spot 9; 118.5 kDa). The largest protein (spot 129, 267.3 kDa) was similar to CHERIO CG3937-PD, isoform D from fruit fly. The smallest protein was LIM protein 1 (spots 166–169; 10.1 kDa). Discrepancies between theoretical and experimental Mr and pI values were found for several proteins. For example, actin was present in 20 different spots, sixteen of which (spots 30–45) had red flour beetle identities (GLEAN_03 326) with the best sequence match (100%) to actin from honey bee. Three spots (46, 47, and 48) corresponding to red flour beetle GLEAN_03944 produced 99% sequence similarity to a putative muscle actin from glassy-winged sharpshooter (*Homalodisca coagulata*). Spot 143 was an NCBI match to actin from honey bee. Although, theoretical Mr/pI values of both red flour beetle proteins were 41.8 kDa/5.3, experimental actin spots were distributed throughout the gel with the most extreme inequality in Mr being around 17 kDa (spots 44 and 45). Another example was a match to red flour beetle GLEAN_06382 protein (spot 108) which, according to calculated theoretical Mr/pI values, is a middle-size basic protein. However, the position on the pronotal 2-D map

rather corresponded to a small slightly acidic protein. The differences between theoretical and experimental Mr/pI could be due to our use of databases from insect species other than SPB. In addition, proteins could have been subjected to robust post-translational processing or digestion with proteases, or protein identification was based on the match to protein's isoform or splice variant. Nonetheless, all actin spots were identified based on fairly high number (9–15) of different peptide matches.

Functional classification

We grouped identified proteins into ten functional categories (Tables 1 and 2). Their biological roles were assigned based on functional annotation of their best matching similar proteins from other insect species. Although the SPB pronotum contained proteins from diverse biological processes and metabolic pathways, five main processes were apparent: metabolism, transport, contractile apparatus, cytoskeleton organization, and defence.

Metabolism. The largest portion of the pronotal proteome was related to metabolism (23% of total identified proteome). Flying insects exhibit some of the highest metabolic rates of O₂ consumption and CO₂ production found in the animal kingdom (Sacktor, 1976). During flight, more than 90% of total organismal O₂ consumption is utilized by thoracic flight muscles (Sacktor, 1976; Rothe & Nachtigall, 1989). Our observations of copious secretion of waxy metabolite into the mycangial lumen and high densities of tracheae for air transfer (Fig. 1) provide additional evidence for high metabolic activity in this region. This group consisted of 22 enzymes from energy-producing pathways involved in metabolism of carbohydrates, lipids, and amino acids. The major sugar breakdown pathways (glycolysis and tricarboxylic acid cycle) were represented with 12 proteins such as mitochondrial aconitase, enolase, fructose-bisphosphate aldolase, isocitrate dehydrogenase, pyruvate dehydrogenase, malate dehydrogenase, NADPH-specific isocitrate dehydrogenase, and triosephosphate isomerase. However, we did not detect a complete set of these enzymes, perhaps due to the unavailability of SPB genomic resources. Amino acid metabolic enzymes consisted of glutamate semialdehyde dehydrogenase, pyrroline-5-carboxylate dehydrogenase, and arginine kinase. Inorganic pyrophosphatase was also included in this category. The presence of enzymes from proline metabolism such as pyrroline-5-carboxylate dehydrogenase and glutamate dehydrogenase indicates that proline may also be a valuable energy substrate for SPB. Different beetle species can indeed preferentially utilize different energy substrates. Carbohydrates are, for instance, preferred energy fuel to proline in the blister beetle (*Decapotoma lunata*; Auerswald & Gade, 1995), while the Colorado potato beetle (*Leptinotarsa decemlineata*) uses

sugars secondary to proline (Mordue & Kort, 1978). It is also important to note that five SPB pronotal proteins responsible for fatty acid/lipid metabolism (trifunctional enzyme beta subunit, 3-hydroxyacyl-CoA dehydrogenase, hydroxyacyl-CoA dehydrogenase, cyclohex-1-ene-1-carboxyl-CoA hydratase, and probable medium-chain specific acyl-CoA dehydrogenase) indicate the importance of lipid oxidation as possible energy source. Based on our observations, we can hypothesize that all three metabolic pathways (carbohydrates, lipids, and amino acids) participate in energy production in the SPB pronotum. Testing this hypothesis requires proper kinetic studies of participating enzymes to distinguish which substrates would be oxidized primarily.

Arginine kinase appears to be an essential pronotal protein, because it was among the highly abundant proteins. Although arginine kinase was present in several spots, spot 56 was one of the most abundant on the gel. The corresponding protein falls into the phosphagen kinase family, catalyzing the reversible phosphorylation of guanidine compounds and yielding ADP and phosphorylated phosphagen (Morrison, 1973). For example, muscle cells retain phosphorylated phosphagen as reservoir of energy that can be quickly released in the form of ATP by backward reaction during the resting period. Since muscle cells exhibit high ATP turnover, this temporary ATP-buffering system allows muscle to generate energy for its contraction immediately (Ellington, 2001). Arginine kinase was identified and characterized in several insects such as the tobacco hornworm (*Manduca sexta*; Rosenthal *et al.*, 1977), Olivier beetle (*Cissites cephalotes*; Tanaka *et al.*, 2007), locust (*Schistocerca gregaria*; Schneider *et al.*, 1989), and American cockroach (*Periplaneta americana*; Sookrung *et al.*, 2006).

Another important energy-related protein was inorganic pyrophosphatase that hydrolyzes inorganic pyrophosphate (PPi) (formed during the ATP-utilizing biosynthetic reactions) to inorganic phosphate. Inorganic pyrophosphatase is a component of nucleosome remodeling factor complex in fruit fly (Gdula *et al.*, 1998), and has potentially similar function in SPB, because it is a highly conserved protein across species in many biosynthetic pathways.

Transport proteins. The second group of identified proteins was those closely related to basic metabolism as well as proteins from coupled mitochondrial ATP synthesis. These were proteins involved in transport, predominantly transport of electrons and protons. The category was composed of 14 proteins (14.6% of all identified proteins). Eight of this class were oxidoreductases, which are commonly involved in electron-transport reactions in various metabolic pathways and/or in maintaining cell redox homeostasis. This category also included ATP synthesis-coupled proton transporting proteins. We identified three membrane subunits (alpha,

beta, and delta) of mitochondrial ATP synthase. Another protein that falls into this category is voltage-gated mitochondrial channel porin which is known to selectively translocate ions and small molecules across the mitochondrial outer membrane (Blachly-Dyson & Forte, 2001).

Muscle and cytoskeleton-related proteins. Proteins from contractile apparatus (14 in all) and cytoskeleton organization (7 in all) constituted another large set of the SPB pronotal proteome. This group of structural proteins represented 22% of all identified proteins. We detected proteins that are major components of both thin and thick muscle filament as well as cell's cytoskeleton. Muscle actin plays an important role in generating contractile force in muscle tissues, and cytoskeletal (non-muscle) actin is a major component of cell structure. For example, the fruit fly genome contains six actin genes: four muscle-specific and two cytoskeletal (Fyrberg *et al.*, 1980, 1983; Tobin *et al.*, 1980, 1990). Nothing is known about actin genes in SPB, and the origin of SPB actin proteins is uncertain. The 16 actin spots (GLEAN_03326) present on pronotal 2-D map might be products of various actin family genes. Alternatively, they could be either isoforms resulting from posttranslational modifications such as glycosylation or phosphorylation, or products of *in vivo* proteolytic cleavage. Troponin and tropomyosin are other important constituents of the thin muscle filament. These proteins are generally present in invertebrates as multiple isoforms. Like actin, tropomyosins can be muscle and non-muscle type of protein. We also identified two out of three troponin subunits: one isoform of calcium-binding troponin C (troponin C2) and two isoforms of actin-binding troponin I (isoforms I-b1 and 6a1). The troponin complex regulates calcium responsive muscular contraction (Farah & Reinach, 1995; Potter *et al.*, 1995).

Proteins that are components of thick filaments of insect muscle were also identified in the SPB pronotum. Both light and heavy chains of myosin were present. These proteins were extensively studied in fruit fly, and at least fifteen myosin heavy chain isoforms were described. All isoforms are alternatively spliced from a single gene, and they are tissue or development specific (reviewed by Morgan, 1995; reviewed by Swank *et al.*, 2000). Two types of myosin light chain proteins are known to exist in invertebrate: the essential and regulatory. Spots 101 and 102 had 71% sequence similarity to myosin light 2 chain, a calcium-binding protein that is potentially involved in regulation. Another thick filament protein present in the SPB pronotum was myofillin. This protein was recently described in fruit fly (Qiu *et al.*, 2005). Further examples of typical muscle proteins were muscle LIM protein, LIM protein 1, and isoforms of 20 kDa muscular proteins. LIM proteins contain conserved cysteine-rich zinc finger domains and are often present in proteins regulating gene expression and cytoskeleton organization and development (Freyd *et al.*, 1990). Two LIM domain

proteins (Mlp60A and Mlp84B) are abundant in fruit fly muscle where they play a role in differentiation of muscle cells (Stronach *et al.*, 1996).

Defence-related proteins. The last abundant category we found included proteins that are known to be involved in organismal defence mechanisms. Stress- and defence-related proteins constituted 16.7% of the total identified SPB pronotal proteome (16 spots). Heat shock proteins (Hsp) such as large (Hsp70 and 60 kDa) and small (Hsp20 family) molecular weight proteins dominated this category as they contributed with eight protein spots. These proteins function as molecular chaperons to ensure proper folding of newly synthesized proteins or refolding of improperly folded proteins. The 70 kDa Hsp family contains two groups of molecular chaperons: heat-inducible and cognate (constitutively expressed). For example, fruit fly possesses five heat-inducible Hsp70 genes, but no cognate member (Holmgren *et al.*, 1979; Craig *et al.*, 1983). The recent analysis of genes encoding Hsp70 in red flour beetle suggests that one was heat-inducible, one constitutive, and the other developmentally regulated (Mahroof *et al.*, 2005). Although the origin of SPB pronotal heat shock proteins is unknown, two out of three 70 kDa Hsp are similar to the cognate members of Hsp70 family. Mitochondrial precursor of 60 kDa Hsp was also present in the SPB pronotal proteome, in addition to several members of the small 20 kDa stress-inducible Hsp family. Stress-responsive peptidyl-prolyl *cis-trans* isomerases accelerate refolding of those denatured proteins that tend to regain their native conformation at very slow rates due to the presence of poorly accessible proline imidic peptide bonds (Fischer & Schmidt, 1990).

We also detected detoxifying enzymes Cu-Zn superoxide dismutase and two thioredoxin peroxidases, which are involved in the antioxidant defence pathways to protect cells from oxidative damage. These enzymes detoxify cells by scavenging the reactive oxygen species that are produced in cells normally or upon numerous environmental stresses. Heat shock proteins and detoxifying enzymes were previously identified in muscle tissues (Yan *et al.*, 2001; Bouley *et al.*, 2004).

Other biological processes. Besides the five functionally dominant groups, the SPB pronotal proteome contained a smaller number of protein representatives from other biological processes. A cluster of 10 proteins (10.4% of total identified proteins) was associated with protein metabolism. The group consisted of three ribosomal proteins (spots 100, 136, and 137) that play a role in protein biosynthesis and of six proteins that appear to be involved in protein catabolism/proteolysis such as subunits of large proteasome complexes from protein degradation machinery (spots 14, 53, 138, and 155), ubiquitin carrier protein (spots 120 and 163), and leucine aminopeptidase (spot 107).

These proteins are part of the cellular degradation machinery and crucial for vitality of every living cell as they are responsible for removal of unfit proteins arisen from mutation, stress, or disease. Moreover, proteolytic enzymes facilitate recycling of amino acids by degrading proteins that are no longer needed.

Among the remaining 13 proteins (13.5% of total identified proteins), a subgroup of proteins were enzymes from metabolism of nucleotides and nucleic acids. Examples include dihydropyrimidinase, nucleoside diphosphate kinase, probable adenylate kinase isoenzyme F38B2.4, and Dak2 protein. Several proteins were related to chromatin remodeling such as high mobility group protein DSP1 and DNA repair protein DNA polymerase iota. A few proteins were related to cellular signaling such as a GTP binding protein (spot 50), receptor for activated protein kinase C-like (spot 86), and guanine nucleotide-binding protein subunit beta-like (spot 66). Last two proteins belong to the WD-repeat (also called beta-propeller) containing family of regulators that carry out a number of biological functions ranging from signal transduction to apoptosis (Smith *et al.*, 1998).

Sub-cellular localization

In addition to functional classification, identified proteins were clustered according to their putative sub-cellular localization (Fig. 3). Only forty six identified proteins (47% of total identified proteins) were assigned a gene ontology (GO) term for cellular component, most of which are associated with mitochondria (10 proteins) and cytoplasm/cytosol (9 proteins). There were few annotated nuclear (4), cytoskeletal (4), intracellular (6), ribosomal (2), and membrane (3) proteins. Eight annotated proteins (8%) are either members of large multi-enzyme complexes such as proton-transporting two-sector ATPase and phosphopyruvate

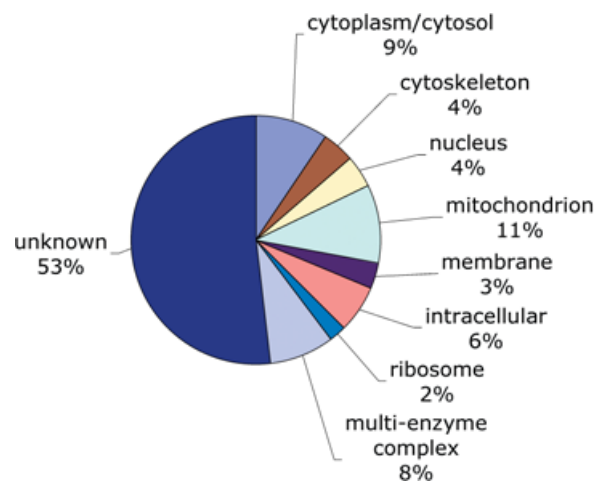


Figure 3. Distribution of identified pronotum proteins according to cellular component of Gene Ontology.

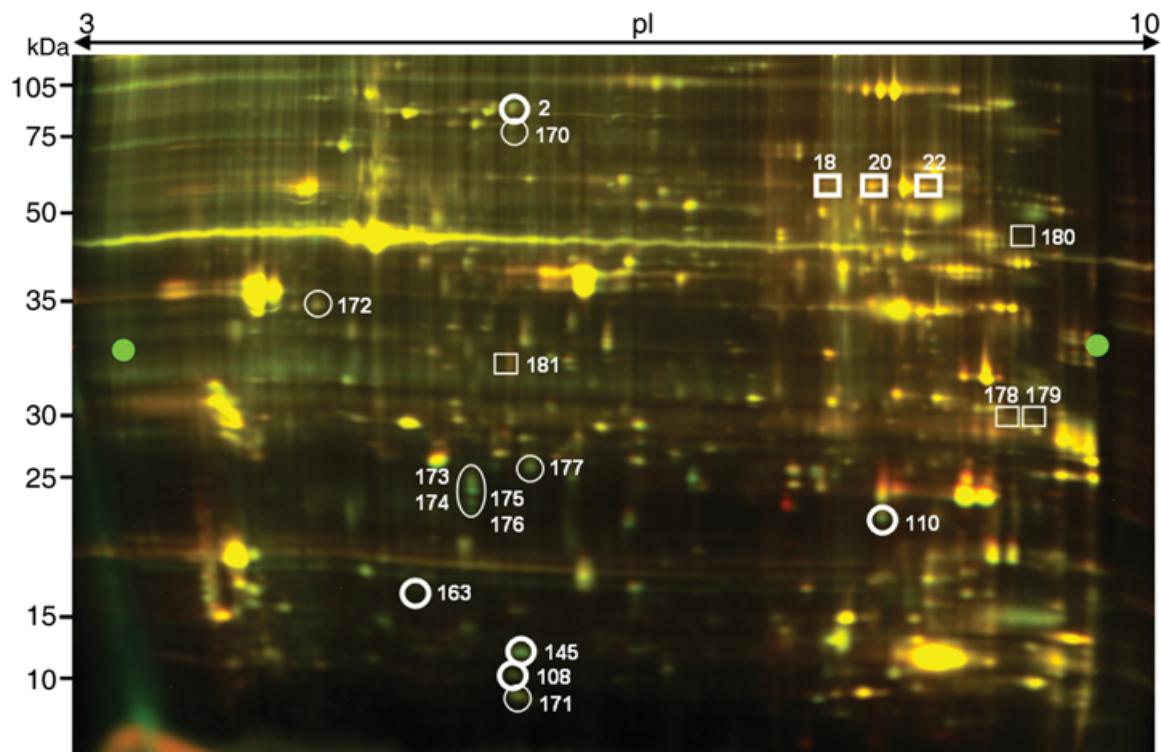


Figure 4. The representative 2-D DIGE overlaid image of Cy3- and Cy5-labeled proteins from female and male pronotum showing differentially expressed proteins. Circled are the proteins that were more abundant in the female pronotum, whereas boxed are the proteins that were more abundant in the male pronotum. Bolded box or circle corresponds to the protein spots that were identified.

hydratase complexes, or components of complex anatomical structures such as striated muscle thick filament and flagellum.

Comparative analysis of female and male SPB pronotal proteomes

One major morphological difference between the SPB sexes is the presence of a well-developed prothoracic mycangium in females (Happ *et al.*, 1971). In *Dendroctonus* and *Xyleborus* spp., the pseudomycangium found in males is reduced and non-functional (Beaver, 1989). The chemical composition and protein profile of mycangia remain unknown. We conducted quantitative proteomic analysis to determine the differences in the pronotum between the sexes with an assumption that differences in protein profiles would reflect the functional mycangium in females. We did not find proteins that qualitatively differed in the pronotum between male and female SPBs, but we did find quantitative differences. A total of 1572 protein spots were detected and visualized on CyDye labeled analytical gels, from which 20 spots showed differential expression ($P < 0.01$; change in spot volume threshold of 1.3) (Fig. 4). Among them, thirteen were more abundant in the female pronotum and seven were more abundant in the male pronotum. We were able to identify only eight of the spots (40%): five in the female pronotum and three in the male

pronotum (Table 3). Three of the female abundant spots (174, 175, and 176) were not present on the preparative gels, and could not be analyzed.

Ubiquitin carrier protein is a component of ubiquitin-conjugating system that catalyzes one of the reactions leading to ubiquitination of proteins targeted for selective degradation (Haas & Bright, 1985). As higher metabolic activity is anticipated within the female mycangial gland cells, increased levels of proteins from ubiquitin-mediated proteolysis are likely needed to regulate turnover of proteins arisen from their abundant synthesis. Ubiquitination also mediates some other cellular processes, such as DNA repair and cell cycle (Jentsch *et al.*, 1987; Goebel *et al.*, 1988), and these processes might be very active within the female mycangial system as it contains high density of glandular cells and mycangial muscles. The elevated levels of two other proteins (75 kDa subunit of NADH-ubiquinone oxidoreductase and GA20735-PA from ATP synthesis and cell redox homeostasis maintenance) might be associated with high energy production due to increased metabolic rate. Muscle 20-like protein belongs to the calponin family with the conserved calponin homology domain, which regulates smooth muscle contraction via binding to actin and other structural muscle proteins (Winder & Walsh, 1993). Higher levels of this protein in the female pronotum

Table 3. List of proteins that are differentially expressed in the female and male SPB pronotum

Spot number	Protein ID <i>Tribolium</i> or NCBI nr database	Expression fold difference	Annotation/protein similarity	Sequence similarity*	Accession number	Organism	Putative function
Proteins more abundant in female pronotum							
2	GLEAN_06252	1.3	NADH-ubiquinone oxidoreductase 75 kDa subunit	72%	Q16LR5	<i>Aedes aegypti</i>	ATP synthesis
110	GLEAN_07135	2.6	Muscle protein 20-like protein	88%	Q4PLJ5	<i>Anoplophora glabripennis</i>	muscle contraction
163	PREDICTED: similar to bendless CG18319-PA, gij66564615 <i>Apis mellifera</i>	1.3	Ubiquitin carrier protein	98%	Q1HQ36	<i>Bombyx mori</i>	protein modification
145	Profilin, gij56404766/Q68HB4	2.3				<i>B. mori</i>	actin filament remodeling
108	GLEAN_06382	2.2	GA20735-PA	60%	Q28XR2	<i>Drosophila pseudoobscura</i>	electron transport, cell redox homeostasis
170	unidentified	1.5					
171	unidentified	2.2					
172	unidentified	1.4					
173	unidentified	2.4					
174	unidentified—not presented on prep gel	3.3					
175	unidentified—not presented on prep gel	3.1					
176	unidentified—not presented on prep gel	4.4					
177	unidentified	1.5					
Proteins more abundant in male pronotum							
18	GLEAN_08728	1.4	Mitochondrial ATP synthase alpha subunit	90%	Q7PHI8	<i>Anopheles gambiae</i> str. PEST	ATP synthesis
20	GLEAN_08728	1.5	Mitochondrial ATP synthase alpha subunit	90%	Q7PHI8	<i>A. gambiae</i> str. PEST	ATP synthesis
22	GLEAN_08728	1.5	Mitochondrial ATP synthase alpha subunit	90%	Q7PHI8	<i>A. gambiae</i> str. PEST	ATP synthesis
178	unidentified	1.5					
179	unidentified	1.6					
180	unidentified	1.3					
181	unidentified	1.8					

*Sequence similarity between red flour beetle protein or unknown NCBI protein and similar protein in UniProtKB.

is perhaps due to presence of mycangial muscles that are absent in males. Profilin, a low molecular weight eukaryotic protein, regulates assembly of actin filaments shaping the structure of cell's cytoskeleton. At high concentration, protein binds to actin monomers preventing their polymerization into filaments (Carlsson *et al.*, 1977). At low concentrations, it enhances actin polymerization. In plants, profilins appear to be associated with resistance to pathogens as they regulate density of actin filaments at the site of pathogen attack to reorganize cytosolic content and facilitate defence (Takemoto *et al.*, 2003). The role of profilin is also important during cell cycle when actin cytoskeleton undergoes vigorous rearrangement. Profilin is essential for posterior patterning of the oocyte during oocytosis in insects (Manseau *et al.*, 1996) and for cytokinesis in yeast (*Saccharomyces cerevisiae*; Chang *et al.*, 1997). Profilin might play a similar role in the female mycangial gland cells.

Although we currently do not have direct evidence that the more abundant proteins in the female SPB pronotum are involved in the synthesis/secretion of chemicals/nutri-

ents, their possible roles should not be dismissed. These proteins could be parts of pathways regulating fungal growth and/or reproduction or be involved in selection against non-symbiotic fungi. They may also be expressed as a part of mycangial self-maintenance.

Three identified proteins that were more abundant in the male pronotum were isoelectric isoforms (the same molecular mass but slightly different pI values) of the same red flour beetle protein, which had 90% sequence similarity to mitochondrial ATP synthase alpha subunit from mosquito. The subunit is part of an enzyme that synthesizes ATP, and its higher expression indicates an increase in ATP synthesis in the male pronotum. However, it is unknown why the male pseudomycangium or pronotum requires more energy. The same protein was up-regulated in the head of honey bee after infection with bacteria (Scharlaken *et al.*, 2007), perhaps due to induced ATP-dependent defences.

Other proteins that might potentially be involved in mycangial gland-specific functions in SPB are listed in

Table 4. List of the southern pine beetle pronotum proteins that are similar to proteins in gland cells of other species. SignalP and TargetP were used to determine the presence of a signal peptide

Pronotum southern pine beetle	Signal peptide	Silk gland silkworm (Zhang <i>et al.</i> , 2006)	Salivary gland female mosquito (Kalume <i>et al.</i> , 2005)	Accessory gland male fruit fly (Walker <i>et al.</i> , 2006)	Mammary gland mouse (Davies <i>et al.</i> , 2006)	Salivary gland human (Hu <i>et al.</i> , 2005)
Enolase	no	Heat shock 70 kDa protein	Enolase	Isocitrate dehydrogenase	Isocitrate dehydrogenase	Alpha enolase Fructose-bisphosphate aldolase
Fructose-bisphosphate aldolase	no					
Isocitrate dehydrogenase	no					
Malate dehydrogenase	no					
HSP 70	no					
Heat shock cognate 70	yes	Heat shock 70 kDa protein	NAD-dependent malate dehydrogenase HSP 70 superfamily	Malate dehydrogenase Heat shock protein 70 kDa	Isocitrate dehydrogenase	Alpha enolase Fructose-bisphosphate aldolase
Peptidyl-prolyl cis-trans isomerase	yes					
Myosin heavy chain, nonmuscle or smooth muscle	no	Actin, cytoplasmic	Contains actin domain	Peptidyl-prolyl cis-trans isomerase	Myosin alpha heavy chain, cardiac muscle	Actin alpha 1
Actin	no					
Putative muscle actin	no					
40S ribosomal protein S12	no					
Ribosomal protein S15e	no					
GTP binding protein	no	ATP synthase beta chain	ATP synthase alpha/beta family	Proteasome subunit alpha type7	Proteasome subunit alpha type1	GTP binding protein ARD 1
ATP synthase subunit beta	no					
Proteasome subunit alpha	no					

Table 4, even though they were not among the differentially expressed proteins. Possible reasons that we did not detect these proteins in our differential proteomic experiments include that these proteins might express below the detection level, or they indeed do not differ in abundance between the sexes. Nonetheless, similar proteins were found in gland cells of other organisms such as silkworm (Zhang *et al.*, 2006), mosquito (Kalume *et al.*, 2005), fruit fly (Walker *et al.*, 2006), mouse (Davies *et al.*, 2006), and human (Hu *et al.*, 2005). This indicates that functions of some proteins are perhaps evolutionarily related in glandular cells across species. These proteins are involved in energy producing metabolism of carbohydrates (e.g. enolase, fructose-bisphosphate aldolase, isocitrate dehydrogenase, and ATP synthase), signaling (e.g. GTP binding protein), or defence (e.g. Hsp70, Hsc70). Indeed, abundant presence of tracheoles within the gland cells of SPB (Fig. 1) indicates high cellular respiration, lending evidence for energy requirement via carbohydrate metabolism. Two proteins (Hsp70 and peptidyl-prolyl cis-trans isomerase) possess signal peptides, but we don't know whether they are targeted to the mycangium or the surrounding gland cells. Therefore, these proteins deserve further functional characterization to determine whether they are involved in gland-cell functions in SPB.

Further investigation of the additional unidentified proteins might increase our understanding of how the mycangium and its surrounding gland cells function. Although some of the proteins were abundant on the 2-D gels (global proteome profile), we did not obtain identification after multiple attempts. These unidentified target proteins may not be well conserved among insects, or may be expressed at low levels that cannot be detected by proteomic-based approaches. However, these proteins might represent novel mycangium-specific proteins that are not present in current databases. As new genomic resources for SPB and/or phylogenetically close species become available, such identifications may become more feasible. We have been using red flour beetle genomic resources for protein identification, because it is the only Coleoptera species whose genome sequencing is in progress. However, SPB and red flour beetle are distantly related, and their families [Scolytidae (Wood, 2007) and Tenebrionidae] diverged 192–228 million years ago (McKenna & Farrell, unpublished). The two beetles also occupy different habitats. SPB is a conifer phloem and fungus-feeding beetle, whereas red flour beetle feeds on milled grain products such as flour and cereals and does not possess mycangia (nor, likely, any mycangium-related genes). Indeed, insect protein sequences generally exhibit strong polymorphism and very high population divergence (Zdobnov *et al.*, 2002; Schevchenko *et al.*, 2005). The Coleoptera order is the most taxonomically and phylogenetically diverse of all the eukaryotic orders. Although

13 961 Coleoptera protein sequences were available in UniProtKB (August, 2007), only five of the best matching proteins were from Coleoptera, and none of them was associated with bark beetles.

In conclusion, we provided the first characterization of SPB pronotal proteome and the identification of candidate proteins for functional genomics. These may serve as potential targets for management of this important forest pest which is difficult to control by conventional means. If any particular pathway within a female SPB mycangium leading to synthesis/secretion of fungus beneficial chemicals/nutrients is altered, this may result in the disruption of the symbiosis and subsequent larval growth and beetle proliferation. Although, not quite to the point of target protein identification, we do provide a first insight into the biochemical make up of the SPB mycangium, an organ which plays a crucial role in the life cycle of SPB. As new genomic resources become available from SPB and/or phylogenetically close species with mycangia, we expect to identify the remaining proteins to increase our understanding of SPB pronotum/mycangium function.

Experimental procedures

Tissue collection

In 2005, a naturally infested site with SPB was located in DeSoto National Forest near Hattiesburg, Mississippi USA. Bolts (80 cm) from the lower bole of infested loblolly pine (*Pinus taeda*) trees were cut, and emergent adult SPB beetles were collected in laboratory. The beetles were sexed under a microscope based on the presence (female) or absence (male) of a pronotal mycangium (Wood, 1982) and the presence (in males) of a groove on the head. Following the removal of head and abdomen, pronotal tissues were collected separately from male and female beetles and immediately frozen in liquid nitrogen. Six replications of male and female tissues were independently sampled. Fifty pronota from either males or females were pooled for each replication. Thus, we dissected a total of at least 600 beetles. Tissues were either fixed for microscopic examination or stored at -80°C for protein extraction.

Scanning electron microscopy

Pronotal tissues were fixed in half-strength Karnovsky's fixative (2% paraformaldehyde and 2.5% glutaraldehyde) with phosphate buffer (0.1 M, pH 7.2) for 48 h at 4°C (Karnovsky, 1965). Specimens were cryo-fractured in liquid nitrogen and dehydrated through a graded ethanol series and stored in 100% ethanol. They were critical-point dried in a Polaron E3000 Critical Point Dryer (Quorum Technologies, Newhaven, UK) using liquid CO_2 . The tissues were then mounted on stubs and coated with gold-palladium using a Polaron E5100 sputter coater (Quorum Technologies). Samples were subsequently examined with a JSM-6500F scanning electron microscope (JEOL, Tokyo, Japan).

Transmission electron microscopy

Pronotal tissues were post-fixed in 2% OsO_4 in 0.1 M phosphate buffer for 2 h, rinsed in distilled water, and dehydrated in a graded

ethanol series. Specimens were infiltrated and embedded in Spurr's resin and polymerized at 70°C for 15 h. Thin sections (60–100 nm) were obtained using an ultramicrotome (Leica Microsystems, Bannackburn, IL), mounted on 50 mesh or single slot copper grids, and double stained with uranyl acetate and lead citrate. At least ten sections were examined and photographed with a JEOL 100 CX II TEM (JEOL) at 80 kV.

Protein extraction from pronotal tissues

Total proteins were independently extracted from six pools (three males and three females) of fifty pronota using a phenol-based procedure with modifications (Hurkman & Tanaka, 1986). Frozen pronota were ground in liquid nitrogen and 1 ml of cold extraction buffer (0.9 M sucrose, 0.5 M Tris-base, 0.05 M $\text{Na}_2\text{-EDTA}$, 0.1 M KCl, 2% β -mercaptoethanol, pH 8.7) into fine powder. One millilitre of cold Tris-saturated phenol (pH 8.0) was added, and the sample was homogenized by shaking for 10 min. The homogenate was centrifuged at 8000 *g* for 30 min. The phenol phase was collected, and one millilitre of extraction buffer was added. Homogenization and centrifugation were repeated. Proteins were precipitated from phenol with five volumes of methanol solution (100% methanol, 0.1 M ammonium acetate and 1% β -mercaptoethanol) at -80°C overnight. Precipitated proteins were collected by centrifugation at 8000 *g* for 10 min and washed three times with cold methanol solution and three times with cold 80% acetone. Proteins were air-dried and stored at -20°C .

Two-dimensional polyacrylamide gel electrophoresis

Proteins were dissolved in sample buffer (9.5 M urea, 1% DTT, 4% CHAPSO and 0.2% ampholines [0.16% ampholine pH 5–10, and 0.04% ampholine pH 3–10]), and concentration was determined using 2-D Quant Kit (Amersham Biosciences, Piscataway, NY). Five hundred micrograms of combined male and female pronotal proteins (250 μg each) were loaded on 24-cm long immobilized pH gradient (IPG) strips with non-linear 3–10 pH range (Bio-Rad, Hercules, CA), and isoelectric focusing (IEF) was carried out using PROTEAN IEF CELL (Bio-Rad, Hercules, CA). Samples were actively rehydrated at 20°C for 12 h, and focusing was performed at 20°C for a total of 80 000 V-hours. Focused IPG strips were equilibrated for 20 min in 6 M urea, 0.375 M Tris-HCl (pH 6.8), 2% SDS, 20% glycerol, 5% β -mercaptoethanol, and Bromphenol Blue. Samples were then loaded onto large format (20 cm \times 20.5 cm \times 1.5 mm) second dimension precast gels (Jule Biotechnologies, Inc., Milford, CT) with 10–15% polyacrylamide gradient and 5% stacking gel and overlaid with 1% agarose. Electrophoresis was carried out in horizontal PROTEAN Plus Dodeca Cell unit (Bio-Rad, Hercules, CA) at 20 mA/gel. Running buffer contained 0.025 M Tris, 0.192 M glycine, 0.001 M EDTA, and 0.2% SDS, pH 8.3. Proteins were visualized by staining with Deep Purple Total Protein Stain (Amersham Biosciences) according to manufacturer's instructions. The gels were scanned using Typhoon 9410 imager (Amersham Biosciences) and analyzed by PDQuest (Bio-Rad). Three replicate gels of mixed female and male pronotal proteins (1:1) were used for proteome profiling.

Two-dimensional differential gel electrophoresis (2-D DIGE)

Proteins were dissolved in 100 μl of sample buffer (8 M urea, 4% CHAPSO, and 30 mM Tris-HCl pH 8.5), and quantified with 2-D Quant Kit (Amersham Biosciences). Three replicates of protein

extracts from male and female beetles were used for the 2-D DIGE experiment. Protein samples were labelled with minimal fluorescent CyDyes such that fifty micrograms of female pronotal proteins were labeled with Cy3, whereas fifty micrograms of male pronotal proteins were labeled with Cy5. Fifty micrograms of internal standard were labeled with Cy2. To prepare the internal standard, a pool of equal amounts (8.34 µg) of six protein samples (three males and three females) was used to normalize abundance of proteins between the gels and control the gel-to-gel variation. Four hundred picomols of CyDye were added to each fifty micrograms of protein sample during labeling, and the mixture was incubated on ice, in dark for 30 min. One microliter of 10 mM lysine was added to each sample, and incubation continued for another 10 min. For each analytical gel, fifty micrograms of Cy3-labeled female pronotal proteins, fifty micrograms of Cy5-labeled male pronotal proteins, and fifty micrograms of Cy2-labeled internal standard were pooled (a total of 150 µg of proteins), and sample/rehydration buffer (9.5 M urea, 1% DTT, 4% CHAPSO, and 0.2% ampholines [0.16% ampholine pH 5–10 and 0.04% ampholine pH 3–10]) was added to the final volume of 440 µl. For preparative gels, two hundred fifty micrograms of unlabeled female pronotal proteins and two hundred fifty micrograms of unlabeled male pronotal proteins were mixed with sample/rehydration buffer to the final volume of 440 µl.

One hundred fifty micrograms of Cy3/Cy5/Cy2-labeled protein samples for analytical gels and five hundred micrograms of unlabeled protein samples for preparative gels were independently loaded on 24-cm long immobilized pH gradient (IPG) strips with non-linear 3–10 pH range (Bio-Rad). IEF was carried out using PROTEAN IEF CELL (Bio-Rad). Samples were actively rehydrated at 20 °C for 12 h, and focusing was performed at 20 °C for a total of 80 000 V-hours. Focused IPG strips were equilibrated for 20 min in 6 M urea, 0.375 M Tris-HCl (pH 6.8), 2% SDS, 20% glycerol, 5% β-mercaptoethanol, and Bromphenol Blue. Samples were then loaded onto large format (25 cm × 20.5 cm × 1.0 mm) second dimension precast gels (Jule Biotechnologies, Inc.) with 10–15% polyacrylamide gradient and 5% stacking gel and overlaid with 1% agarose. Electrophoresis was carried out in horizontal PROTEAN Plus Dodeca Cell unit (Bio-Rad) at 20 mA/gel. Running buffer contained 0.025 M Tris, 0.192 M glycine, 0.001 M EDTA, and 0.2% SDS, pH 8.3. Preparative gels were stained with Deep Purple Total Protein Stain (Amersham Biosciences) according to manufacturer's instructions.

Gel imaging and data analysis for 2-D DIGE experiment

Analytical and preparative gels were scanned using Typhoon 9410 imager (Amersham Biosciences). For analytical gels, excitation/emission wavelengths were 532 nm/580 nm for Cy3, 633 nm/670 nm for Cy5, and 488 nm/520 nm for Cy2. Preparative gels were excited at 532 nm, and emission spectra were filtered through 560 LP general filter. All scans were acquired at 100 µm resolution. For data analysis, images of analytical gels were processed using Batch Processor module of DECYDER™ software V5.0 (Amersham Biosciences), which includes Difference In-gel Analysis (DIA) for intra-gel spot detection and Biological Variation Analysis (BVA) for cross-gel statistical analysis to obtain relative quantization of protein spot volumes. Student's T-test and one-way analysis of variance (ANOVA) were used to calculate significant differences in protein abundances between female and male pronota ($P < 0.01$). Images of female and male analytical gels as well as their overlaid two-colour images are shown in Fig. 5.

In-gel digestion and mass spectrometry

Protein spots (global proteome profiling) and differentially expressed protein spots exhibiting at least 1.3-fold change in protein expression were excised from Deep Purple stained gels using Spot Picker (Amersham Biosciences) and subjected to automated in-gel digestion on ProPrep robotic digester (Genomic Solutions, Ann Arbor, MI) using sequencing grade modified trypsin (Promega, Madison, WI). Resulting peptides were desalted with C18 ZipTips and spotted on MALDI plate in 70% ACN, 0.1% TFA and 5 mg/ml matrix (α-cyano-4-hydroxycinnamic acid).

Mass spectra were collected using the ABI 4700 MALDI TOF/TOF mass spectrometer (Applied Biosystems, Foster City, CA). Protein identification (ID) was performed using the Result Dependent Analysis (RDA) of ABI GPS Explorer V3.5 software. MS peak filtering was set at 800–4000 m/z interval, minimum S/N at 10, and mass tolerance at 150 ppm. MS/MS peak filtering was monoisotopic, minimum S/N was set at 3, and MS/MS fragment tolerance was set at 0.2 Da. After an initial MS scan, data were analyzed as peptide mass fingerprinting (PMF), and preliminary protein ID was conducted through a search against the National Center for Biotechnology Information (NCBI) and red flour beetle protein databases using the MASCOT algorithm (Pappin *et al.*, 1993). Proteins with high confidence ID (Cross Confidence Interval C.I. % > 95%) were automatically selected for *in silico* digestion. For their 1st RDA (top protein confirmation), the three strongest corresponding peptides/parent ions in the MS spectra were selected for MS/MS analysis. For the sample spots not yielding high confidence, preliminary PMF ID were subjected to 2nd RDA during which first fifteen strongest parent ions from MS spectra were subjected to MS/MS. The spectral data form PMF (initial MS scan), 1st and 2nd RDA were analyzed together in combined MASCOT search against the red flour beetle or NCBI database.

Protein identification and comparative sequence analysis

Protein identification was performed using two protein databases. First, the MS/MS spectra were searched against the red flour beetle protein database (<http://www.hgsc.bcm.tmc.edu/projects/tribolium/>) to obtain GLEAN protein identities and protein sequences. MS/MS searches that did not yield positive identification in the red flour beetle database were matched against the NCBI non-redundant database. For NCBI searches, taxonomy was limited to Insecta, Coleoptera, and fruit fly. For both databases, MS/MS hits with total protein score C.I. % > 95% were considered as a positive identification. At the time of query the red flour beetle database contained 16 422 protein sequences which produced 3 906 304 peptides following *in silico* digestion with trypsin (3 558 882 unique peptide identifiers). The red flour beetle protein sequences were further used in BLAST searches against UniProt Knowledgebase (<http://www.pir.uniprot.org/search/blast.shtml>) using BLOSUM62 algorithm and an E value cut-off of 1.0×10^{-5} to find similar proteins for annotation. For each red flour beetle protein ID, the best matching sequence was considered as protein identification/similarity. The same was performed for unknown or predicted proteins using the NCBI matches.

For functional classification, identified proteins were assigned a putative biological process based on Gene Ontology Annotation (GOA) of their best matching similar protein sequences in the UniProt database. Proteins that did not have assigned GO term for biological process were classified according to GOA of protein's Protein Information Resource SuperFamily (PIRS). Classification

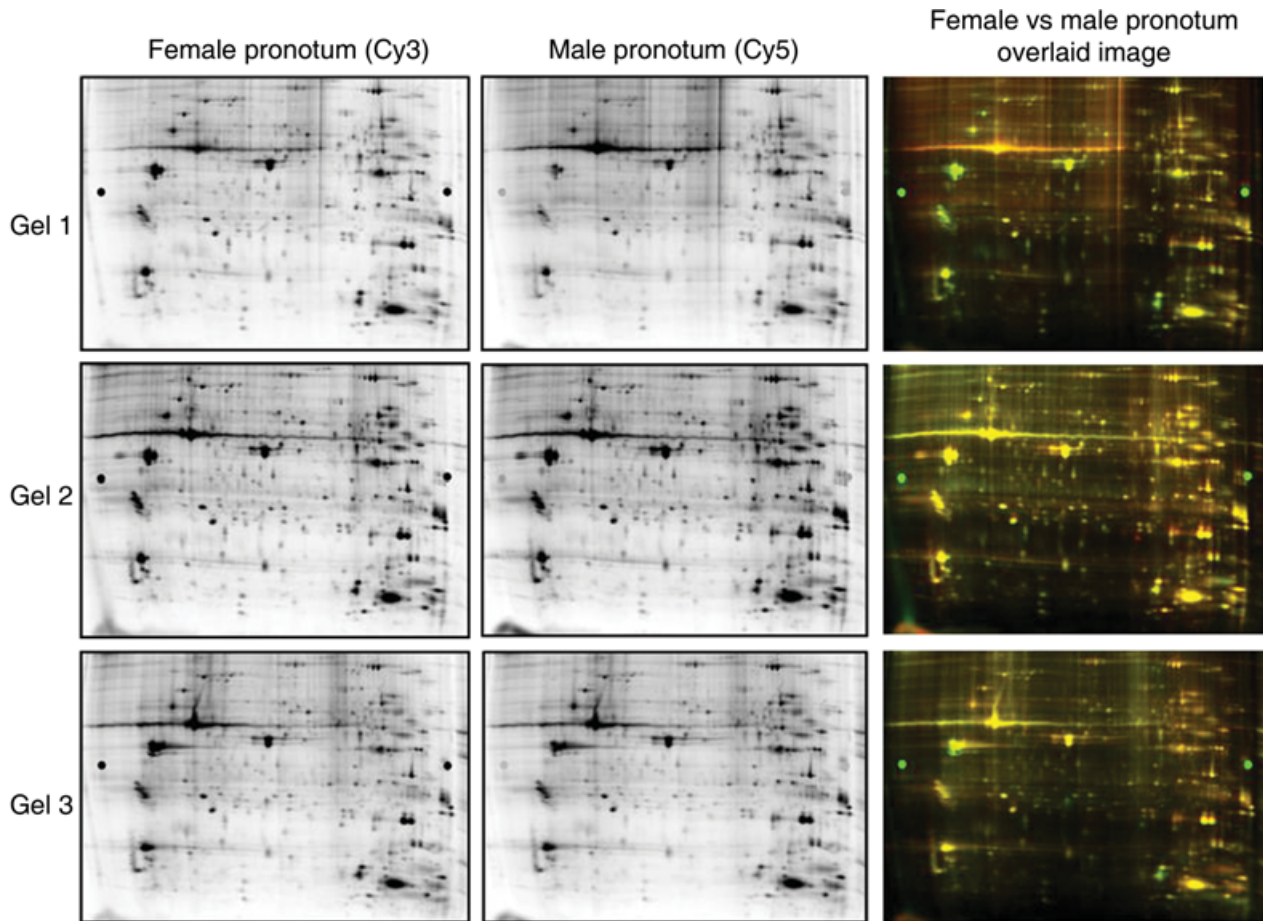


Figure 5. 2-D analytical maps of Cy3-labeled female pronotum proteins, Cy5-labeled male pronotum proteins, and their overlaid colored images from 2-D DIGE experiments (Cy2-labeled images of internal standards not shown).

from UniProt Gene Ontology Annotations (GOA) was used for cellular compartment.

The identified SPB proteins using the red flour beetle protein database were screened against the proteins that are present in gland cells of other species. The matching proteins were then screened for the presence of signal peptides and prediction of subcellular location using TargetP (<http://www.cbs.dtu.dk/services/TargetP>) (Emanuelsson *et al.*, 2000) and SignalP (<http://www.cbs.dtu.dk/services/SignalP>) (Nielsen *et al.*, 1997) algorithms.

Acknowledgements

We thank the *Tribolium* Genome Sequencing Consortium, the Baylor College of Medicine Human genome sequencing center, Erich Vallery at the USDA Forest Service, Southern Research Station, and Tibor Pechan at the MSU Life Sciences and Biotechnology Institute. This project was supported by the USDA Forest Service, Southern Research Station.

References

- Adams, M.D., Celniker, S.E., Holt, R.A., Evans, C.A., Gocayne, J.D., Amanatides, P.G. *et al.* (2000) The genome sequence of *Drosophila melanogaster*. *Science* **287**: 2185–2195.
- Auerswald, L. and Gade, G. (1995) Energy substrates for flight in the Blister beetle, *Decapotoma lunata* (Meloidae). *J Exp Biol* **198**: 1423–1431.
- Barras, S.J. and Perry, T.J. (1972) Fungal symbionts in the prothoracic mycangium of *Dendroctonus frontalis*. *Zeitschrift Angew Entomologie* **71**: 95–104.
- Barras, S.J. and Taylor, J.J. (1973) Varietal Ceratocystis minor identified from Mycangium of *Dendroctonus frontalis*. *Mycopathologica et Mycologia Applicata* **50**: 203–305.
- Beaver, R.A. (1989) Insect-fungus relationship in the bark and ambrosia beetles. In *Insect-Fungus Interactions* (Wilding, N., Collins, N.M., Hammond, P.M. and Webber, J.F., eds), pp. 121–134. Academic Press, San Diego, California.
- Biron, D.G., Ponton, F., Marche, L., Galeotti, N., Renault, L., Demey-Thomas, E. *et al.* (2006) 'Suicide' of crickets harbouring hairworms: a proteomics investigation. *Insect Mol Biol* **15** (6): 731–742.
- Blachly-Dyson, E. and Forte, M. (2001) VDAC channels. *J Int Union Biochem Mol Biol Life* **52**: 113–1180.
- Bouley, J., Chambon, C. and Picard, B. (2004) Mapping of bovine skeletal muscle proteins using two-dimensional gel electrophoresis and mass spectrometry. *Proteomics* **4**: 1811–1824.
- Carlsson, L., Nystrom, L.E., Sundkvist, I., Markey, F. and Lindberg, U. (1977) Actin polymerizability is influenced by profilin, a low

- molecular weight protein in non-muscle cells. *J Mol Biol* **115**: 465–483.
- Chang, F., Drubin, D. and Nurse, P. (1997) cdc12p, a protein required for cytokinesis in fission yeasts, is a component of the cell division ring and interacts with profilin. *J Cellular Biol* **137**: 169–182.
- Craig, E.A., Ingolia, T.D. and Manseau, L.J. (1983) Expression of heat shock cognate genes during heat shock and development. *Dev Biol* **99**: 418–426.
- Davies, C.R., Morris, J.S., Griffiths, M.R., Page, M.J., Pitt, A., Stein, T. *et al.* (2006) Proteomic analysis of the mouse mammary gland is a powerful tool to identify novel proteins that are differentially expressed during mammary development. *Proteomics* **6**: 5694–5704.
- Drooz, A.T. (1985) *Insects of Eastern Forests*. U.S. Department of Agriculture, Forest Service Miscellaneous Publication 1246, Washington, D.C. 608 p.
- Ellington, W.R. (2001) Evolution and physiological roles of phosphagen systems. *Annu Rev Physiol* **63**: 289–325.
- Emanuelsson, O., Nielsen, H., Brunak, S. and von Heijne, G. (2000) Predicting subcellular localization of proteins based on their N-terminal amino acid sequence. *J Mol Biol* **300**: 1005–1016.
- Farah, C.S. and Reinach, F.C. (1995) The troponin complex and regulation of muscle contraction. *FASEB J* **9**: 755–767.
- Fischer, G. and Schmidt, F.X. (1990) The mechanism of protein folding. Implications of in vitro refolding models for de novo protein folding and translocation in the cell. *Biochemistry* **29**: 2205–2212.
- Freyd, G., Kim, S.K. and Horvitz, H.R. (1990) novel cysteine-rich motif and homeodomain in the product of the *Caenorhabditis elegans* cell lineage gene lin-11. *Nature* **244**: 876–879.
- Fyrberg, E.A., Kindle, K.L., Davidson, N. and Kindle, K.L. (1980) The actin genes of *Drosophila*: a dispersed multigene family. *Cell* **19**: 365–378.
- Fyrberg, E.A., Mahaffey, J.W., Bond, B.J. and Davidson, N. (1983) Transcripts of six *Drosophila* actin genes accumulate in a stage- and tissue-specific manner. *Cell* **33**: 115–123.
- Gdula, D.A., Sandaltzopoulos, R., Tsukiyama, T., Ossipov, V. and Wu, C. (1998) Inorganic pyrophosphatase is a component of the *Drosophila* nucleosome remodeling factor complex. *Genes Dev* **12**: 3206–3216.
- Goebel, M.G., Yochern, J., Jentsch, S., McGrath, J.P., Varshavsky, A. and Byers, B. (1988) The yeast cell cycle gene CDC34 encodes a ubiquitin-conjugating enzyme. *Science* **241**: 1331–1335.
- Haas, A.L. and Bright, P.M. (1985) The immunochemical detection and quantitation of intracellular ubiquitin-protein conjugates. *J Biol Chem* **260**: 12464–12473.
- Happ, G.M., Happ, C.M. and Barras, S.J. (1976) Bark beetle-fungal symbiosis. Fine Structure of a basidiomycetous ectosymbiont of the southern pine beetle. *Can J Bot* **54**: 1049–1062.
- Happ, G.M., Happ, C.M. and Barras, S.J. (1971) Fine structure of the prothoracic mycangium, a chamber for the culture of symbiotic fungi, in the southern pine beetle, *Dendroctonus frontalis*. *Tissue Cell* **3**: 295–308.
- Holmgren, R., Livak, K., Morimoto, R., Freund, R. and Meselson, M. (1979) Studies of cloned sequences from four *Drosophila* heat shock loci. *Cell* **18**: 1359–1370.
- Holt, R.A., Subramanian, G.M., Halpern, A., Granger, G., Sutton, I., Charlab, R. *et al.* (2002) The genome sequence of the malaria mosquito *Anopheles gambiae*. *Science* **298**: 129–149.
- Hsiao, P.T.W. and Harrington, T.C. (1997) *Ceratocystopsis brevicornis* sp. Nov., a mycangial fungus of *Dendroctonus brevicornis* (Coleoptera: Scolytidae). *Mycologia* **89**: 661–669.
- Hsiao, P.T.W. and Harrington, T.C. (2003) Phylogenetics and adaptations of Basidiomycetous fungi fed upon by bark beetles (Coleoptera: Scolytidae). *Symbiosis* **34**: 111–131.
- Hu, S., Xie, Y., Ramachandran, P., Ogorzalek Loo, R.R., Li, Y., Loo, J.A. *et al.* (2005) Large-scale identification of proteins in human salivary proteome by liquid chromatography/mass spectrometry and two-dimensional gel electrophoresis-mass spectrometry. *Proteomics* **5**: 1714–1728.
- Hurkman, W.J. and Tanaka, C.K. (1986) Solubilization of plant membrane proteins for analysis by two-dimensional gel electrophoresis. *Plant Physiol* **81**: 802–806.
- Jacobs, K. and Kirisits, T. (2003) *Ophiostoma kryptum* sp. nov. from *Larix decidua* and *Picea abies* in Europe, similar to *O. minus*. *Mycol Res* **107**: 231–242.
- Jentsch, S., McGrath, J.P. and Varshavsky, A. (1987) The yeast DNA repair gene *RAD6* encodes a ubiquitin-conjugating enzyme. *Nature* **329**: 131–134.
- Kalume, D.E., Okulate, M., Zhong, J., Reddy, R., Suresh, S., Deshpande, N. *et al.* (2005) A proteomic analysis of salivary glands of female *Anopheles gambiae* mosquito. *Proteomics* **5**: 3765–3777.
- Karnovsky, M.J. (1965) A formaldehyde-glutaraldehyde fixative of high osmolarity for use in electron microscopy. *J Cell Biol* **27**: 137A–138A.
- Klepzig, K.D., Moser, J.C., Lombardero, M.J., Hofstetter, R.W. and Ayres, M.P. (2001) Symbiosis and competition: Complex interactions among beetles, fungi and mites. *Symbiosis* **30**: 83–96.
- Lefevre, T., Thomas, F., Schwartz, A., Levashina, E., Blandin, S., Brizard, J.-P. *et al.* (2007) Malaria *Plasmodium* agent induces alteration in the head proteome of their *Anopheles* mosquito host. *Proteomics* **7**: 1908–1915.
- Mahroof, R., Zhu, K.Y., Neven, L., Subramanyam, B. and Bai, J. (2005) Expression patterns of three heat shock protein 70 genes among developmental stages of the red flour beetle, *Tribolium castaneum* (Coleoptera: tenebrionidae). *Comp Biochem Physiol, Part A* **141**: 247–256.
- Manseau, L., Calley, J. and Phan, H. (1996) Profilin is required for posterior patterning of the *Drosophila* oocyte. *Development* **122**: 2109–2116.
- Mordue, W. and de Kort, C.A.D. (1978) Energy substrates for flight in Colorado beetle, *Leptinotarsa decemlineata* Say. *J Insect Physiol* **24**: 221–224.
- Morgan, N.S. (1995) The myosin superfamily in *Drosophila melanogaster*. *J Exp Zool* **273**: 104–117.
- Morrison, J.F. (1973) Arginine kinase and other invertebrate guanidine kinases. In *The Enzymes* (Boyer, P.D., ed.), pp. 457–486. Academic Press, New York.
- Nielsen, H., Engelbrecht, J., Brunak, S. and von Heijne, G. (1997) Identification of prokaryotic and eukaryotic signal peptides and prediction of their cleavage sites. *Protein Eng* **10**: 1–6.
- Pappin, D.J.C., Hojrup, P. and Bleasby, A.J. (1993) Rapid identification of proteins by peptide mass fingerprinting. *Curr Biol* **3**: 327–332.
- Potter, J.D., Sheng, Z., Pan, B.S. and Zhao, J. (1995) A direct role for troponin T and a dual role for troponin C in the Ca²⁺ regulation of muscle contraction. *J Biol Chem* **270**: 2557–2562.

- Pye, J.M., Price, T.S., Clarke, S.R. and Huggett, Jr., R.J. (2004) A History of Southern Pine Beetle Outbreaks in the Southeastern United States through 2004. Web publication: <http://www.srs.fs.usda.gov/econ/data/spb/index.htm>
- Qiu, F., Brendel, S., Cunha, P.M.F., Astola, N., Song, B., Furlong, E.E.M. *et al.* (2005) Myofilin, a protein in the thick filaments of insect muscle. *J Cell Sci* **118**: 1527–1536.
- Rosenthal, G.A., Dahlman, D.L. and Robinson, G.W. (1977) L-Arginine kinase from tobacco hornworm, *Manduca sexta* (L.). Purification, properties, and interaction with L-cavananine. *J Biol Chem* **252**: 3679–3683.
- Rothe, U. and Nachtigall, W. (1989) Flight of the honeybee. IV. Respiratory quotients and metabolic rates during sitting, walking and flying. *J Comp Physiol* **158**: 739–749.
- Sacktor, B. (1976) Biochemical adaptations for flight in the insect. *Biochem Soc Symp* **41**: 111–131.
- Santos, K.S., dos Santos, L.D., Mendes, M.A., de Souza B.M., Malaspina, O. and Palma, M.S. (2004) Profiling the proteome complement of the secretion from hypopharyngeal gland of Africanized nurse-honeybees. *Insect Biochem Mol Biol* **35**: 85–91.
- Scharlaken, B., de Graaf, D.C., Memmi, S., Devreese, B., Van Beeumen, J. and Jacobs, F.J. (2007) Differential protein expression in the honeybee head after a bacterial challenge. *Arch Insect Biochem Physiol* **65**: 223–237.
- Schevchenko, A., de Sousa, M.M.L., Waridel, P., Bittencourt, S.T., de Sousa, M.V. and Schevchenko, A. (2005) Sequence similarity-based proteomics in insects: characterization of the larvae venom of the Brazilian moth, *Cerodirpha speciosa*. *J Proteome Res* **4**: 862–869.
- Schneider, A., Wiesner, R.J. and Grieshaber, M.K. (1989) On the role of arginine kinase in insect flight muscle. *Insect Biochem* **19**: 471–480.
- Smith, T.F., Gaitatzes, G., Saxena, K. and Neer, E.J. (1998) The WD repeat: a common architecture for diverse functions. *Trends Biochem Sci* **24**: 181–185.
- Sookrung, N., Chaicumpa, W., Tungtrongchir, A., Vichyanond, P., Bunnag, C., Ramasoota, P. *et al.* (2006) *Periplaneta americana* arginine kinase as a major cockroach allergen among thai patient with cockroach allergies. *Environ Health Perspect* **114**: 875–880.
- Stronach, B.E., Seigrist, S.E. and Beckerle, M.C. (1996) Two muscle-specific LIM proteins in *Drosophila*. *J Cell Biol* **134**: 1179–1195.
- Swank, D.M., Wells, L., Kronert, W.A., Morrill, G.E. and Bernstein, S.I. (2000) Determining structure/function relationship for sarcomeric myosin heavy chain by genetic and transgenic manipulation of *Drosophila*. *Microsc Res Tech* **50**: 430–442.
- Takemoto, D., Jones, D.A. and Hardham, A.R. (2003) GFP-tagging of cell components reveals the dynamics of subcellular reorganization in response to infection of *Arabidopsis* by oomycete pathogen. *Plant J* **33**: 775–792.
- Tanaka, K., Ichinari, S., Iwanami, K., Yoshimatsu, S. and Suzuki, T. (2007) Arginine kinase from the beetle *Cissites cephalotes* (Olivier). Molecular cloning, phylogenetic analysis and enzymatic properties. *Insect Biochem Mol Biol* **37**: 338–345.
- The Honey Bee Genome Sequencing Consortium (2006) Insight into social insects from the genome of the honeybee *Apis mellifera*. *Nature* **433**: 931–949.
- Tobin, S.L., Cook, P.J. and Burn, T.C. (1990) Transcripts of individual *Drosophila* actins are differentially distributed during embryogenesis. *Dev Genet* **11**: 15–26.
- Tobin, S.L., Zulauf, E., Sanchez, F., Craig, E.A. and McCarthy, B.J. (1980) Multiple actin-related sequences in the *Drosophila melanogaster* genome. *Cell* **19**: 121–131.
- Walker, M.J., Rylett, C.M., Keen, J.N., Audsley, N., Sajid, M., Shirras, A.D. *et al.* (2006) Proteomic identification of *Drosophila melanogaster* male accessory gland proteins, including a pro-cathepsin and soluble γ -glutamyl transpeptidase. *Proteome Sci* **4**: 9–18.
- Winder, S.J. and Walsh, M.P. (1993) Calponin: thin filament-linked regulation of smooth muscle contraction. *Cell Signal* **5**: 677–686.
- Wood, S.L. (1982) The bark and ambrosia beetles of North and Central America (Coleoptera: Scolytidae), a taxonomic monograph. *Great Basin Nat Mem* **6**: 1–1359.
- Wood, S.L. (2007) *Bark and Ambrosia Beetles of South America (Coleoptera, Scolytidae)*. Brigham Young University, M.L. Bean Life Science Museum, Provo, Utah, 900 pp.
- Yan, J.X., Harry, R.A., Wait, R., Welson, S.Y., Emery, P.W., Preedy, V.R. *et al.* (2001) Separation and identification of rat skeletal muscle proteins using two-dimensional gel electrophoresis and mass spectrometry. *Proteomics* **1**: 424–434.
- Zdobnov, E.M., von Mering, C., Letunic, I., Torrens, D., Suyama, M., Copley, R.R. *et al.* (2002) Comparative genome and proteome analysis of *Anopheles gambiae* and *Drosophila melanogaster*. *Science* **298**: 149–159.
- Zhang, P., Aso, Y., Jikuya, H., Kusakabe, T., Lee, J.M., Kawaguchi, Y. *et al.* (2007) Proteomic profiling of the silkworm skeletal muscle proteins during larval-pupal metamorphosis. *J Proteome Res* **6**: 2295–2303.
- Zhang, P., Aso, Y., Yamamoto, K., Banno, Y., Wang, Y., Tsuchida, K. *et al.* (2006) Proteome analysis of silk gland proteins from the silkworm, *Bombyx mori*. *Proteomics* **6**: 2586–2599.